jove

Two-Photon Polymerization 3D-Printing of Micro-scale Neuronal Cell Culture Devices

Ali Hosseini[1], **Giovanni Noselli**[2], **Michele Giugliano**[1]

[1] Neuroscience Department, International School for Advanced Studies [2] Mathematics Department, International School for Advanced Studies

Corresponding Author

Michele Giugliano
michele.giugliano@sissa.it

Citation

Hosseini, A., Noselli, G., Giugliano, M. Two-Photon Polymerization 3D-Printing of Micro-scale Neuronal Cell Culture Devices. *J. Vis. Exp.* (208), e66142, doi:10.3791/66142 (2024).

Date Published

June 7, 2024

DOI

10.3791/66142

URL

jove.com/video/66142

Abstract

Neuronal cultures have been a reference experimental model for several decades. However, 3D cell arrangement, spatial constraints on neurite outgrowth, and realistic synaptic connectivity are missing. The latter limits the study of structure and function in the context of compartmentalization and diminishes the significance of cultures in neuroscience. Approximating *ex vivo* the structured anatomical arrangement of synaptic connectivity is not trivial, despite being key for the emergence of rhythms, synaptic plasticity, and ultimately, brain pathophysiology. Here, two-photon polymerization (2PP) is employed as a 3D printing technique, enabling the rapid fabrication of polymeric cell culture devices using polydimethyl-siloxane (PDMS) at the micrometer scale. Compared to conventional replica molding techniques based on microphotolitography, 2PP micro-scale printing enables rapid and affordable turnaround of prototypes. This protocol illustrates the design and fabrication of PDMS-based microfluidic devices aimed at culturing modular neuronal networks. As a proof-of-principle, a two-chamber device is presented to physically constrain connectivity. Specifically, an asymmetric axonal outgrowth during *ex vivo* development is favored and allowed to be directed from one chamber to the other. In order to probe the functional consequences of unidirectional synaptic interactions, commercial microelectrode arrays are chosen to monitor the bioelectrical activity of interconnected neuronal modules. Here, methods to 1) fabricate molds with micrometer precision and 2) perform *in vitro* multisite extracellular recordings in rat cortical neuronal cultures are illustrated. By decreasing costs and future widespread accessibility of 2PP 3D-printing, this method will become more and more relevant across research labs worldwide. Especially in neurotechnology and high-throughput neural data recording, the ease and rapidity of prototyping simplified *in vitro* models will improve experimental control and theoretical understanding of *in vivo* large-scale neural systems.

Introduction

Investigating neuronal activity in behaving organisms presents several challenges. For instance, physical access to the brain tissue is limited by the need to maintain its integrity, so the brain's superficial regions are more easily considered. Isolating specific targets within the intact tissue is often a daunting task and sometimes impossible. Although dissociated homogeneous neuronal cultures offer convenient access to the molecular, biochemical, and biophysical properties of individual (sub)cellular components of a neural circuit, a realistic connectivity and anatomical organization of the intact brain is lost. These fundamental constraints inspired research efforts to achieve a middle ground, where *in vivo* complexity is avoided while the structure can be constructed *in vitro,* which is on demand[1,2,3,4,5,6,7,8,9]. In particular, modular neuronal cultures have been a subject of extensive research over the past decades, aiming to tackle key questions of brain physiology as described below.

Organization: *In vivo* studies show that the brain is structured anatomically in layers with precise cell types and arrays of projections. Functional assays revealed the organization of the neuronal networks in node assemblies and modules, with precise connectivity schemes[10,11]. The role of connectivity and microcircuit motifs cannot, however, be studied adequately *in vivo* due to the sheer number of synapses that are involved, as well as the interwoven effects of development and activity-dependent plasticity.

Signal transfer: In *in vivo* or random *in vitro* cultures, it is challenging to assess signal transfer. Examining the axonal conduction and action potential along its length requires guiding neurite outgrowth by surface functionalization or chemical patterning, providing a high signal-to-noise ratio in extracellular readouts of electrical activity[12].

Translational relevance: Deciphering the exclusive role of pre- versus post-synaptic elements across pathological conditions requires having access to these elements individually. Modular cultures with constrained connectivity, effectively segregating the pre-and post-synaptic elements, are indispensable tools to this end[13].

Several methods exist to obtain some form of structure in neuronal culture. They can be broadly categorized as chemical and physical surface manipulation[9]. The former methods[14,15] rely on the propensity of neuronal cells to attach to certain (bio)chemical compounds. This requires depositing adhesive or attractive molecules on a surface with micro-scale precision and following a detailed pattern. While this allows a partial coverage of the surface of the cells, following the desired pattern, chemical methods are inherently limited and have a relatively low success rate in neurite growth guidance[16]. Full control over axon directionality requires establishing a spatial gradient of ad-hoc chemicals to shape axonal guidance[17]. The latter methods involve physical surface manipulation and are more commonly used to structure the neuronal networks *in vitro*. Neuronal cells are physically constrained at desired locations by geometrical confinements, such as microscopic chambers, walls, channels, etc., shaping a biocompatible polymer such as polydimethylsiloxane (PDMS)[3,5,6,7,18,19,20] cured and solidified into a microfluidic device. The *de facto* method for PDMS microfluidic fabrication is soft photolithography[21], where a two-dimensional mask is patterned at a micro-scale and employed to selectively etch a silicon-based material

upon UV exposure. In a nutshell, a UV-curable resin (i.e., photoresist) is coated onto a silicon wafer through spin-coating, reaching a specific height determined by its viscosity and spinning speed. Then, the patterned mask is positioned over the photoresist and exposed to UV light. Transparent areas within the mask, corresponding to regions of interest, will let UV light induce localized crosslinking of the photoresist molecules. The areas of unexposed photoresist are washed away using a solvent, resulting in the formation of a master mold. This is repeatedly used to bake an elastomer of the choice (i.e., PDMS), which is then engraved with the desired geometries in as many replicas as desired. Such a manufacturing method is the most common method to fabricate microfluidic devices[22]. Perhaps the main limitations of soft photolithography are the prerequisite of notable capital investment and the unfamiliarity of biological labs with the required techniques and expertise. The preparation of the mask and the steps of soft photolithography required to design complex multiple-height high aspect ratio geometries are non-trivial[23] and often require outsourcing. Even though alternative and low-budget methods have been proposed, they do not always satisfy the high precision requirements of biological prototyping[24].

Here, an alternative manufacturing method is presented, relying on two-photon polymerization (2PP) and additive manufacturing. It is straightforward and does not require per se advanced microfabrication and microphotolitography expertise. The research field of 2PP micromanufacture emerged in the late 90's[25], and since then, it has witnessed exponential growth[26]. More about the fundamental principles of this technique can be found elsewhere[26]. Briefly, by focusing the excitation light impulse in three-dimensional space, 2PP leverages the nonlinear dependence of multiphoton absorption on intensity. This grants the capability of confined absorption, ensuring precise and selective excitation within very localized regions. In essence, a negative-tone photoresist, a material with decreased solubility upon light exposure, is subjected to a focused beam of femtosecond laser pulses at a low duty-cycle[27]. This allows for impulses with high intensities at low average powers, enabling polymerization without harming the material. The interaction of photo-induced radical monomers gives rise to radical oligomers, initiating polymerization that extends throughout the photoresist up to a distinct volume, i.e., voxel, whose size depends on the intensity and duration of the laser pulses[28].

In this work, two components are presented: A) the design and rapid fabrication of a 3D-printed mold, reusable many times to produce disposable polymeric neuronal cell culture devices (**Figure 1**), and B) their mechanical coupling onto the surface of planar neuronal cell culture substrates, or even of substrate-integrated microelectrode arrays capable of multisite recordings of bioelectric signals.

Computer Assisted Design of a 3D mechanical model is very briefly described here and accompanied by the steps leading to a 3D-printed mold and fabricating PDMS devices is also detailed.

A variety of computer-aided design software applications can be used to generate the starting 3D object model and produce a STL file to control the 2PP printing process. Within the **Table of Materials**, the first and the last applications listed are free-of-charge or provided with a free license. Constructing a 3D model always requires creating a 2D sketch, which is then extruded in subsequent modelling steps. To demonstrate this concept, a generic 3D CAD software design process is highlighted in protocol section, leading to a structure made of overlapping cubes. For more comprehensive information,

a number of online tutorials and free training resources are available, as indicated in the **Table of Materials**.

The resulting STL file is then translated into a series of commands to be executed by the 3D-printer (i.e., slicing procedure). For the specific 2PP 3D-printer in use, the software DeScribe is used to import the STL file and convert it into the proprietary General Writing Language (GWL) format. The success of 2PP printing process hinges on various parameters, notably, laser power and its scan speed, stitching, and hatching-slicing distances. The choice of these parameters, along with the selection of objective and photoresist, depends on the design's smallest features, as well as the intended application. Thus, parameter optimization becomes essential to meet the requirements of different design scenarios and use cases. For this work, the recommended recipe IP-S 25x ITO Shell (3D MF) has been considered as a configuration for the printing parameters. Ultimately, a mechanically stable printed part is printed with the necessary resolution while minimizing its 3D-printing time.

The mold design and related STL file, demonstrated in this work, comprises a square frame to segregate the space of a cell culture in two compartments: an outer area (i.e., referred to as Source subsequently) and an inner area (i.e., referred to as Target subsequently). These two compartments are connected through sets of microchannels, each characterized by sharp-angle borders, designed to specifically hinder the growth of neurites from the Target to the Source, but not vice versa, and as such promote a directional synaptic connectivity between neurons growing on the two areas.

Earlier studies employed different geometries of microchannels to encourage the directional growth of neurites. Examples include triangular shapes[18], channel barbed structures[19], and tapering channels[20]. Here, a design featuring sharp angle barriers across the microchannel's borders is employed, characterized also by asymmetric entrances. These microchannels serve to establish continuity between an enclosed interior, the Target compartment, and the external area, the Source compartment. The funnel shape of the initial part of the microchannels, from the Source side, is designed to promote the formation of axonal bundles and their growth along the shortest, i.e., straight line, path connecting the Source to the Target. The triangular space realized by facing sharp angles have larger volume at the Target side to aim at effectively delaying neurites' pathfinding while favoring the rapid shooting of bundles originating from the Source and occupation of the available space. The choice of 540 µm for the length of the microchannels effectively filters out the generally shorter dendritic outgrowth[39]. In addition, their 5 µm height prevents cell somata from penetrating through the microchannels. Overall, this configuration proved to promote unidirectional connectivity between the outer, Source, and inner, Target modules, and it is presented here as a proof-of-principle among the many alternative choices.

While the PDMS devices, fabricated by the 2PP mold, can be attached to the surface of common cell culture substrates, such as glass coverslips or Petri dishes, in this work commercially available substrate-integrated microelectrode arrays were used. No effort has been made to optimize the 3D design to the microelectrode array layout, and the mechanical coupling was performed under stereomicroscopy guidance aiming only at positioning the device across the array, leaving some microelectrode uncovered in both sides, the Source and the Target. This enables the preliminary assessment of the functional consequences of the constrained connectivity in neuronal cell cultures.

Protocol

All procedures involving animal handling were carried out in accordance with European and Italian laws (European Parliament and Council Directive of 22 September 2010 [2010/63/EU]; Italian Governmental Decree of 4 March 2014, no. 26), were explicitly approved by the institutional OpBA (Committee for Animal Care) at the Scuola Internazionale Superiore di Studi Avanzati and were officially authorized by the Italian Ministry of Health (Auth. No. 22DAB.N.UVD). These led to the availability of non-sentient material from the explanted rat brain tissue, to be used for the experimental validation of the method presented in this work.

1. 3D mold fabrication by two-photon polymerization

1. Generating the CAD files

   NOTE: The following steps demonstrate a generic 3D design workflow, employing computer aided design software (i.e., SolidWorks). The sample STL design file described in this work (**Figure 2**) is available as **Supplementary Coding File 1**, as well as through Zenodo (https://doi.org/10.5281/zenodo.8222110).

   1. Launch the computer aided design software desktop application. From the top menu bar, select **New**.
   2. From the options, choose **Part: a 3D representation of a single design component**. Press the key combination **Ctrl + 5** to establish the top view of the sketch.
   3. From the side panel, select **Sketch** and choose **Corner Rectangle**. Select one edge of the rectangle by clicking on it. As a parameters panel appears, set the length to 100 units.
   4. Repeat step 1.1.3 for the edge perpendicular to the previous one: set its length to 50 units. Select the rectangle by dragging over it while holding the left mouse button.
   5. From the **Add Relation** menu, select **Fix**, to constrain the relations among lines.
   6. Exit the sketch and repeat steps 1.1.3 to 1.1.5, creating a new (smaller) rectangle, overlapping the previous sketch.
   7. From the side panel, select **Features**, and choose **Extruded Boss/Base**: set the depth of both the large and small rectangles to 5 and 10 unit, respectively.
   8. From **File** menu, save the part in STL format (i.e., Standard Tessellation Language).

2. Processing the CAD files

   1. Transfer the STL file to a personal computer, equipped with the DeScribe application software.
   2. Launch **Describe** and from its File menu, open the STL file. A 3D representation of the model will appear.
   3. From the orientation section on the right-hand side menu, rotate the model to orient it appropriately in space, and center it in the plane.
   4. Adjust the overall scaling by selecting the **Scaling** section of the right-hand side menu.
   5. From the drop-down menu on the top, select the **IP-S 25x ITO Shell (3D MF) recipe**. This specifies IP-S as photoresist, 25x for the magnification power of the objective, Indium Tin Oxide (ITO) coated substrate as printing substrate, and shell and scaffold printing as operating mode with medium-size features (MF).

6. Navigate through the wizard, selecting and setting **Slicing distance** to 1 µm and **Hatching distance** to 0.5 µm for both the shell and the scaffold.
7. In the output step of the import wizard, under splitting, define the block size as X = 200 µm, Y = 200 µm and Z = 265 µm and the block offset as X = 133 µm, Y = 133 µm, and Z = 0, ensuring that the delicate structures of the microchannels are not affected by the stitching lines.
8. As Scan mode, use the default: Galvo for X-Y plane and Piezo for the Z-axis.
9. Press **Save** and, in the next textual menu, replace the line var **$baseLaserPower = $shellLaserPower** with var **$baseLaserPower = 75**, to reduce to 75% the laser power at the lowest layer of the print.
10. Transfer the GWL files obtained by the above steps to the workstation dedicated for 2PP 3D printing.

3. 3D printing and sample development
    1. Launch the **NanoWrite** application software. After printer initialization, click on **Exchange Holder** on the software interface, to insert the substrate holder and mount the objective.
    2. Mount the 25x objective in the appropriate position on the nosepiece. Identify which side of the glass substrate is coated with ITO, by an electronic multimeter set to measure resistances: the reading should be low values, such as 100-300 Ω, but only for the ITO-coated side.
    3. Position the glass substrate on the holder, orienting the ITO-coated side upwards. Use tape to firmly hold it in place.
    4. Under the chemical fume hood, apply a drop of IP-S photoresist at the center of the glass substrate.
    5. Insert the holder into the 3D-printer, with the resin drop facing the objective (i.e., downward).
    6. Through the software **File** menu, load the GWL files. Select **Approach Sample**, to move the objective close to the resin drop.
    7. Select **Find Interface** to allow detection of the ITO-photoresist printing interface, based on the refraction index difference of the two materials.
    8. Select **Start Job** to launch the printing. As printing finishes, press **Exchange Holder** to retrieve the holder.
    9. Retrieve the holder and gently remove the substrate with the printed part. Submerge the glass substrate into propylene glycol methyl ether acetate (PGMEA) for 20 min under the fume hood, to develop the printed part.
    10. Remove the substrate from PGMEA and submerge it in isopropanol for 5 min. Allow the printed part to air dry, under the chemical fume hood.
4. Post-print treatment and mold mounting
    1. Cure the printed part by exposure to UV light (i.e., 365-405 nm) with sufficient power for 5-20 min (see **Discussion** for power details).
    2. Under a laminar flow hood, gently remove the printed part from the glass substrate. Drop ~2 µL of resin to the bottom of a 35 mm x 10 mm Petri dish.
    3. Carefully position the printed part over the drop and let the resin flow beneath the part. Further cure the printed part by exposure to UV light, for 5 min.

4. Cover the Petri dish with its cap and transfer it to the oven for heat curing, over 30 min at 80 °C. Do not preheat the oven to avoid deformation or fracture of the printed part. After curing, the printed part will be permanently attached to the bottom of the Petri dish. From now on, the printed and mounted part will be referred to as mold.

2. PDMS device fabrication from the mold and cell culture substrates

1. PDMS device fabrication
    1. Prepare 20 mL of 10:1 (weight ratio) mixture of the base and curing*agent* of unpolymerized PDMS. For each device, and depending on its required height, 1-2 mL of PDMS mixture is enough. Store the excess unpolymerized PDMS at -20 °C for later use.
    2. Under a laminar flow hood, thoroughly stir the mixture for 4 min. As the mixture traps air bubbles evenly, it will become opaque.
    3. Transfer the mixture into a 50 µL µtube and centrifuge it at 168 x *g* for 5 min, to eliminate air bubbles from the mixture and achieve a clear appearance.
    4. Treat the mold with 10 µL of hydrophobing agent (i.e., Repel-silane ES) and allow it to rest for 7 min, ensuring a smooth detachment of the polymerized PDMS from the mold later on.
    5. Rinse mold 1x with 70% ethanol, and 2x with deionized (DI) water. Allow the mold to air dry under the laminar flow hood.
    6. Gently pour the PDMS mixture onto the mold, until the intended final height of the device is reached. To prevent the formation of air bubbles, pour the mixture gently and from a close distance to the mold's surface.
    7. Cover the mold and transfer it for 18 min to an oven that has been preheated and stabilized at 80 °C, for curing. For device heights more than 5 mm and up to 1 cm, extend the curing time from 18 to 25 min.
    8. Under the laminar flow hood, gently detach the cured PDMS block from the mold and submerge it in isopropanol for at least 10 min, inside a glass Petri dish. Isopropanol eliminates uncrosslinked PDMS. Always keep the PDMS block covered.
    9. Renew the isopropanol and, under a stereo microscope, carefully cut out the central square section of the device (identified as the Target area, in this work) by an ophthalmic stab knife. Then, proceed to further cut along the edges to achieve the device's ultimate shape.
    10. Retrieve the device from isopropanol and submerge it in ethanol for 30 min, and then rinse it 3x with sterile DI water. Maintain sterility from this point onward.
    11. Under a laminar flow hood, transfer the device into a new Petri dish, leaving its cap slightly open. Allow it to air dry completely.
2. Device mounting and cell culture substrates preparation.
    1. Sterilize each microelectrodes arrays (MEAs) by submerging in 70% ethanol for 30 min, and then rinse it 3x with sterile DI water.
    2. Using sterile fine tweezers, under a laminar flow hood and stereomicroscope, mount the PDMS device onto the inner area of a MEA. Align one side of the PDMS device to the center of the inner MEA area, featuring substrate-integrated

microelectrodes, so that few microelectrodes are left uncovered from both Source and Target areas (see **Figure 2**).

NOTE: For this work, it is not necessary to align MEA microelectrodes to the PDMS device microchannel. A gentle push on the device may be required to achieve a tight seal between the PDMS device and the MEA surface. Avoid at all costs to touch the microelectrodes by the tweezers' tip.

3. Insert the MEA with PDMS device on it into the plasma cleaner chamber, to activate the surface activation through air plasma. Begin the process with a 4 min vacuum pump evacuation of the chamber. Next, open the air valve slightly to allow controlled air bleeding. Close the air valve and switch on the plasma inducers, adjusting the RF power level between 10 W and 18 W.
4. Once a glowing light appears, let the process run for 80 s. Then, switch off the plasma inducer, close the vacuum pump valve, and gently open the air valve. Open the chamber to retrieve the MEA.

   NOTE: If the plasma treatment involves exposing MEAs to a non-sterile environment, place each MEA under UV light in a laminar flow hood for 30 min, to ensure the sterility.
5. Add 1 mL of polyethyleneimine (PEI) 0.1% wt/vol solution to the MEA and incubate it at 37 °C overnight. Aspirate the PEI solution and rinse with sterile DI water 5x. Add 1 mL of the cell culture medium to the MEA and incubate it prior to cell seeding.

3. Neuronal cell culture and electrophysiology

1. Prepare in advance the dissection medium, the digestion solution, and the solutions 1-3 (see **Table 1**).
2. Dissociated neuronal cell culture.
   1. Gently grasp a neonatal Wistar rat pup aged 0-1 days by the snout and perform rapid decapitation using a sharp pair of scissors.
   2. Peel off the scalp skin, make an incision along the sagittal mid-line of the skull using fine scissors, and then create a coronal cut through the skull at the junction of the cerebellum.
   3. Remove the skull, scoop out the brain with a fine spatula and transfer it to cold (4 °C) dissection medium.
   4. Remove the subcortical tissue, hippocampus, and meninges. Mince the tissue into small pieces (i.e., 1-2 mm^3) and transfer them in a 15 mL tube. Discard the solution and rinse the tissue using fresh dissection medium, followed by a wash with digestion medium.
   5. Discard the digestion medium, then add 1 mL of Solution 1. Incubate the mixture at 37 °C for 5 min. Discard solution 1 and rinse the tissue with fresh dissection medium. Then add 1 mL of solution 2 and keep the mixture for 10 min at 4 °C.
   6. Discard solution 2 and rinse the tissue using fresh dissection medium. Then add 1 mL of solution 3. Mechanically dissociate the cells by slowly pipetting up and down the solution 20 to 30 times. As a uniformly turbid mixture of dissociated cells appears,

raise its volume to 3 mL by adding dissection medium.

7. Collect the cell pellet by centrifuging the mixture at 100 x *g* for 5 min. Aspirate the supernatant and resuspend the cell pellet in 1 mL of pre-warmed culture medium.

8. Count cells (i.e., by a cell-counting chamber) and adjust the density of the cell seeding solution accordingly.

9. Seed each MEA with 1 mL of seeding solution with the nominal cell density of 1.8 x 10^6 (~ 6500 cells/mm^2). Incubate the seeded MEAs in a humid incubator at 37 °C and 5% CO_2. Exchange the medium with fresh (i.e., weekly made) culture medium every 2 days.

3. Extracellular electrophysiology

NOTE: Dissociated neuronal cell cultures reach a fully mature electrical phenotype after 2-3 weeks *in vitro*. The following sections describe an extracellular stimulation protocol using a commercial MEA application software (Experimenter) to electrically stimulate either of the neuronal populations cultured in modules, i.e., Source or Target, while simultaneously recording the activity of both populations, in mature networks.

1. Gently mount one MEA inside the headstage of the multichannel electronic amplifier, inside a dry incubator (37 °C, 5% CO_2) and allow it to accommodate for 10 min. A custom PDMS cap may be fabricated separately and used as a tight cover for each MEA, to reduce water evaporation and maintain sterility.

2. Launch the Experimenter software. Set the sampling rate to 25 kHz and start data acquisition by pressing **Start DAQ**. In the Data Display panel, the raw traces of extracellularly recorded activity for each channel appear.

3. Monitor the spontaneous activity and visually identify and select 3 pairs of neighboring microelectrodes that are active during bursts of network-wide spontaneous synchronized activity bursts, either from the Source or Target side microelectrodes.

4. In the stimulator panel of the software, configure the parameters for each of the stimulating microelectrode pairs in bipolar configuration: select a biphasic pulse waveform and set the peak amplitudes to ± 800 mV, and the pulse duration to 200 µs.

5. Set the recorder and record for a period of 300 ms before to 1000 ms after the stimulation.

6. Repeat step 3.3.3 to 3.3.5 for the Source and the Target side in an interleaved fashion for the required number of repetitions.

Representative Results

The fabrication of a 2-compartment polymeric (neuronal) cell culture device is reported here, exemplifying the use of 2PP 3D-printing for rapid prototyping of PDMS devices. Specifically, a device is produced for modular neuronal networks with unidirectional synaptic connectivity and its functional characterization is presented in terms of multisite extracellular electrophysiology. Briefly, a micrometer scale mold was realized by means of direct laser writing, using a commercially available 3D printer. In particular, the printer delivers a power of 50 mW through laser pulses with center wavelength of 780 nm and a duration of 80 to 100 fs. During the fabrication process, the laser beam is focused through

the objective (25x, NA=0.8) of the printer onto the negative-tone photoresist (IP-S) to scan the printing volume using the galvo scanner for the x and y axes, and the piezo stage for the z axis. The printing volume was suitably split in blocks of 200 mm x 200 mm x 265 mm to realize a mold with overall size of 6500 mm x 6500 mm x 545 mm and nominal volume of 12.423 mL. **Figure 2A** represents a 2D sketch of the mold, highlighting its dimensions and features' size, whereas **Figure 2B** shows a close-up photo of the finished device mounted on a MEA. The molds prepared as described in the previous section were durable and could be reused more than 50 times to fabricate PDMS devices.

The printed mold was used for casting the PDMS device, which was then mounted on the inner area of glass-substrate integrated arrays of microelectrodes arrays (MEA), to be used for multisite extracellular recordings of neuronal electrical activity and as a proof-of-principle. Commercial substrate-integrated MEAs were used to monitor the activity of modular cultures in response to spatially localized electrical stimuli delivered extracellularly by a subset of microelecrode located in each culture compartment. Each MEA contains 120 Titanium nitrate (TiN) microelectrodes with a diameter of 30 µm and 100 µm inter-electrode pitch. **Figure 2C-D** shows the placement of the PDMS device on the top of the MEA. The geometrical features of individual microchannels of the device together with the overall footprint of the chamber shown in **Figure 2C**, lead to a compartmentalization of the cultured neurons. These can be distinguished based on the compartment they belong to, in the outer area (Source) of the device, or in the inner area (Target) of the device. The preferred axonal guidance, restricted from the Source to the Target, is dictated by the sharp-angled edges of the microchannels. **Figure 2D** shows the placement of the polymeric device on the MEA and the relative coverage area of recording electrodes located within the Source or the Target compartments. Note that a precise alignment of the inside of device's microchannels to one or more rows of MEA microelectrodes was neither required for our case-study nor pursued.

Representative evidence of asymmetric neurite growth is provided in **Figure 3**, during *ex vivo* development, showing fluorescently tagged neurites in live imaging, 6 days (**Figure 3A**) and 2 days following cell plating (**Figure 3B-D**). While the neurites on the Target side of the device encountered sharp angle barriers as obstacles impeding their progression through space, the neurites originating from the Source side grew uninterrupted and crossed the channels. This asymmetry favors a unidirectional axonal connection between neurons in the two compartments, projecting from Source to Target, as explicitly intended from the design. This result is further supported by a (functional) electrophysiological evaluation of electrical responses evoked by stimuli alternatively delivered in each of the two compartments.

After 3-4 weeks *in vitro*, as neuronal networks reached full maturity[29,30], the functional connectivity across the two compartments could be probed upon delivering brief electrical stimuli and monitoring the neuronal responses they evoked[31]. Biphasic electrical impulses with an amplitude of 800 mV were then applied alternatively only to the Source or only to the Target populations (N repetitions = 150, N modular cultures = 6), delivered by 3 juxtaposed pairs of planar microelectrodes in a bipolar configuration, and in an interleaved fashion. Therefore, the 3 pairs of electrodes could be located within the Source area of the MEA or within the Target area of the MEA. The electrical responses evoked by each stimulus could be then detected by all

MEA microelectrodes after a propagation delay. Recordings were performed with a sampling rate of 25 kHz/channel, and the resulting extracellular raw electrical signals were digitized at an analog-to-digital conversion resolution of 16 bits. A threshold crossing peak-detection algorithm[32] was used offline to detect the time of occurrences of extracellular action potentials, without performing any spike sorting. **Figure 4A-B** clearly unveil a strong asymmetry of evoked responses, repeated 150 times, depending on the location of the stimulus delivery, suggesting a significant functional impact of the geometrical constraints on the preferred directionality of connectivity. In fact, upon stimulating the Source side, the firing rate of the Source neuronal population - estimated by computing the peri-stimulus spike-times histogram - increased as expected generating a full network-burst of action potentials[33,31,34] and it was followed, after a delay, by an increase in firing rate of the Target population. However, as the stimulation was delivered within the Target population, only the firing rate of the Target population increased with the Source population remaining mostly silent. **Figure 4C-D** repeats the same stimulus/response paradigm in a control culture, with no polymeric device present (i.e., an unstructured neuronal culture), the extracellular stimuli were also delivered over 4 repetitions. For such control conditions, no asymmetry occurred in the responses evoked by either stimulus. While the subset of MEA microelectrodes used to deliver the stimuli matched that used in modular networks, the location of the stimulus delivery led to a similar evoked response from the entire population. This confirms that the PDMS device favored unidirectional synaptic connectivity, across the two compartments. Overall, asymmetric responses evoked in modular cultures (N = 6) and symmetric responses evoked in control cultures (N = 4) strongly indicate a constrained anatomical connectivity of a compartmentalized *in vitro* system. The electrophysiological data and the scripts used to generate **Figure 4**, are made available through Zenodo (https://doi.org/10.5281/zenodo.8220990).

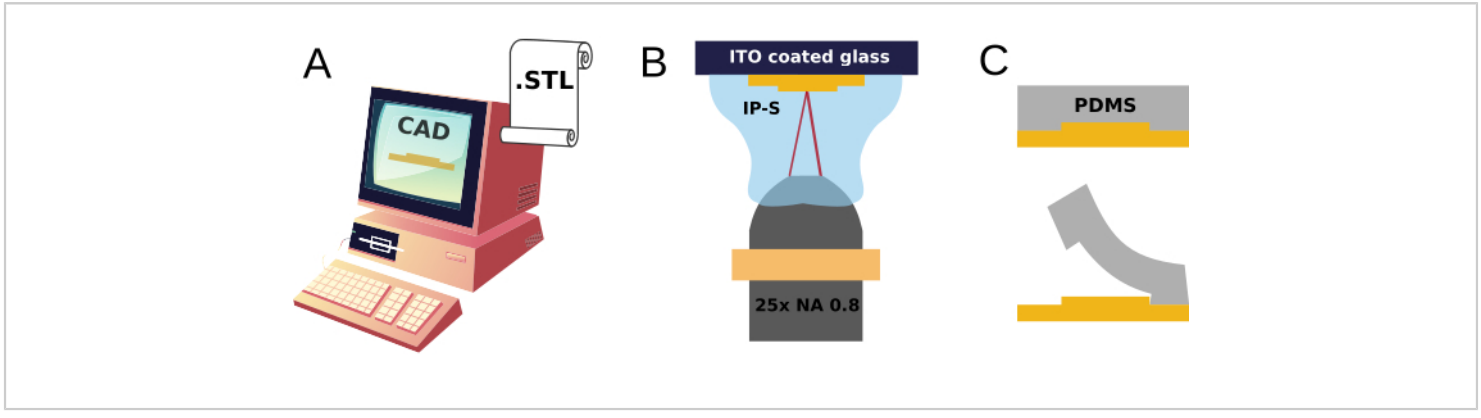

Figure 1: Sketch of the 2PP micro-mold manufacture and PDMS replica molding. (A) A 3D model is designed in CAD and exported in Standard Tessellation Language (STL) format file, **(B)** instructing its 2-photon 3D-printing through laser-induced polymerization within a drop of resin (IP-S). **(C)** The resulting structure is used as a mold for repeated fabrication of PDMS replicas. Please click here to view a larger version of this figure.

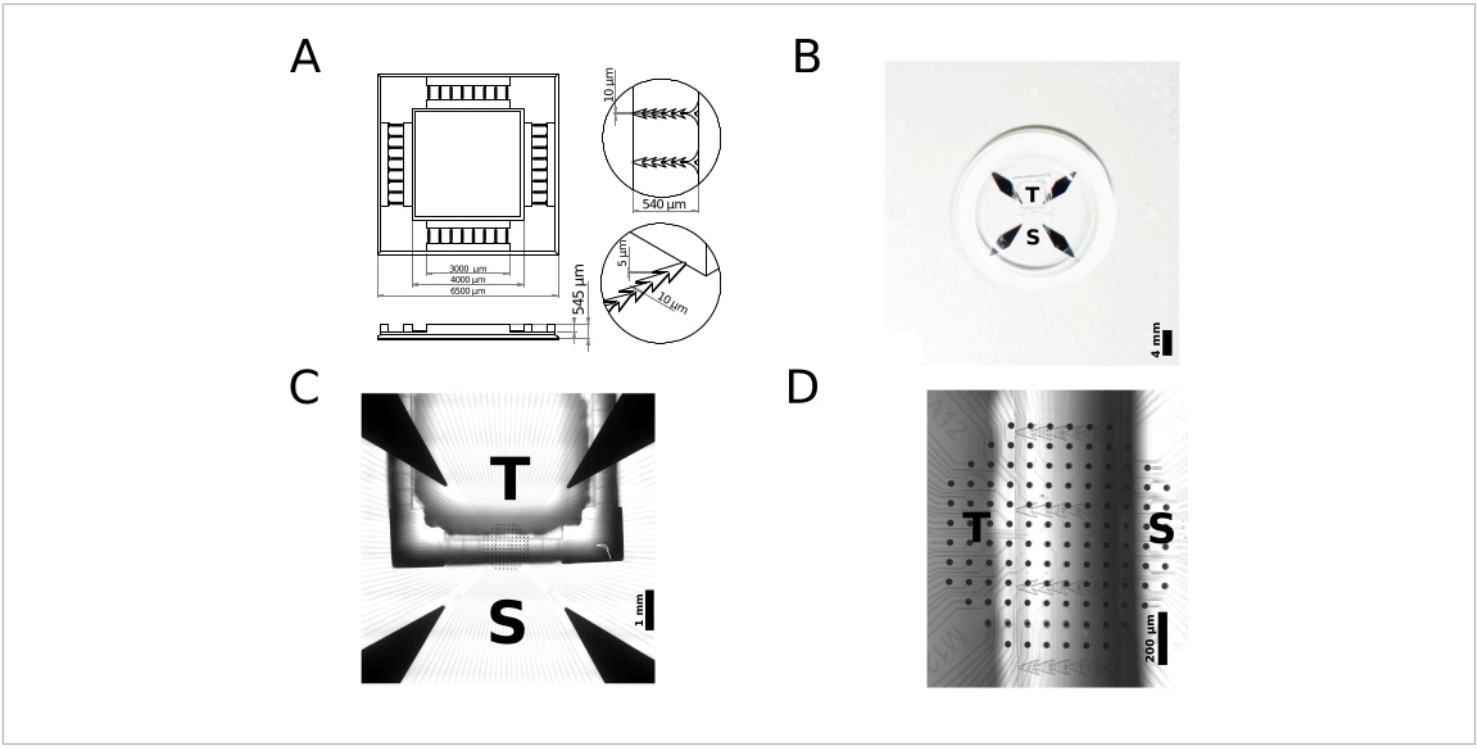

Figure 2: Example of in-house rapid prototyping of a polymeric (neuronal) cell culture PDMS device. (A) In less than 24 h, micro-scale additive manufacturing allows going from a CAD model to a 3D-printed master, to be used immediately, and repeatedly, as a replica mold with biocompatible elastomers, such as PDMS. **(B-C)** The resulting PDMS devices are coupled to a neuronal cell culture planar substrate, here represented by an array of microelectrodes. For the specific sample design in **(A)**, two chambers are defined: one referred to as Source and indicated by S, and the other referred to as Target and indicated by T. **(D)** Neurons plated in each chamber can only grow their neurites through a series of microchannels. When aligned appropriately under stereo microscopy guidance in **(C)**, two sets of substrate-integrated microelectrodes are left exposed, so that the bioelectrical activity of nearby neurons located in both compartments can be stimulated and recorded. Note here that aligning microelectrodes within individual microchannels was not the priority of this proof-of-principle. Please click here to view a larger version of this figure.

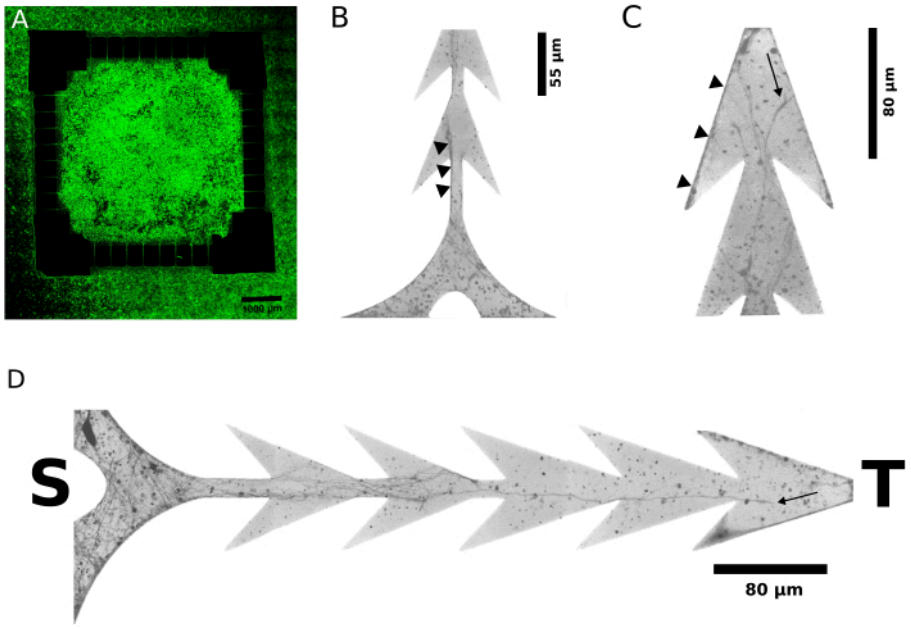

Figure 3: Live imaging of cell-impermeant fluorescent reporter molecules, identifies neurites elongated by neurons, few days after cell plating. (A-D) Representative confocal fluorescence micrographs of modular neuronal cultures of the device fabricated from **Figure 1** and **Figure 2** (N = 4, 128 individual microchannels) have been acquired 2 and 6 days after cells plating. **(B-D)** The 40x magnification and an inverted gray scale of the micrographs for increased visibility. The endings of the microchannels from the Source and the Target compartments are denoted by S and T, respectively. **(A)** shows the wide-scan image of the culture, where Source (i.e., the inner square area) and Target (i.e., the outer area) are full of cells, 6 days after plating. **(B)** and **(C)** display, at the earlier time point of 2 days after plating, the growth of neurites at the Source and at the Target sides of the microchannels, respectively. The small black triangles indicate representative examples of putative axon bundles terminals, apparently originating only from the Source. The arrow shaped microchannels' boundaries point to the elongation of neurites along the edge **(B)**, where their passage is uninterrupted and guided towards the Target. In the opposite direction, and next to the Target ending of a microchannel **(C),** neurites originating from the Target and advancing to the Source side are entrapped at the sharp corners. **(D)** further reveals the details of neurite outgrowth inside a microchannel. Please click here to view a larger version of this figure.

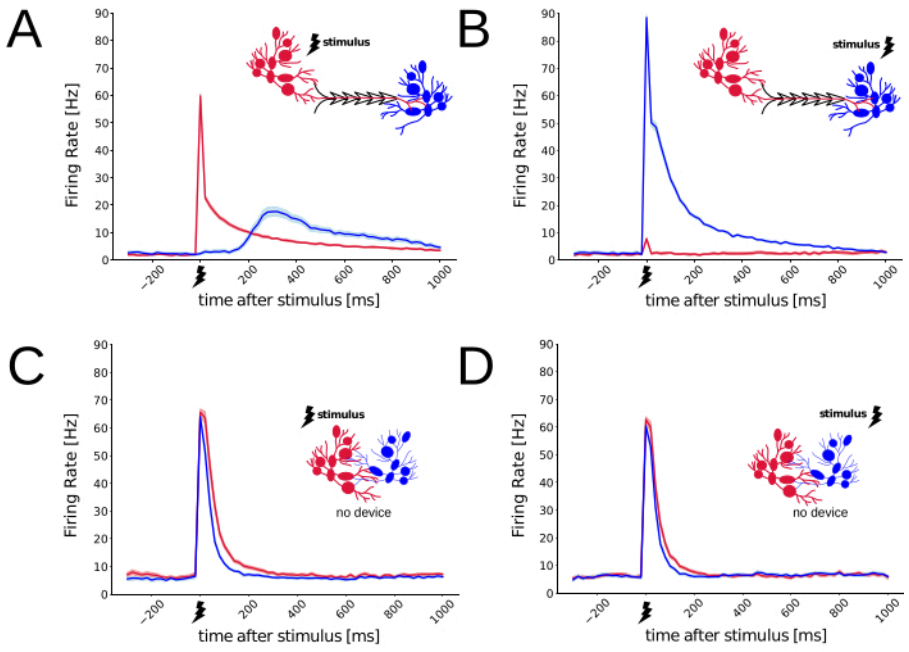

Figure 4: Functional characterization of neuronal electrical responses, with and without the PDMS device. MEAs were used as cell culturing substrates and employed to measure the network-wide spiking responses evoked by a very brief (i.e., 200 µs, 0.8V) biphasic electrical stimulation pulse, delivered in a bipolar configuration. With the PDMS device of **Figure 2**, the neuronal spiking responses recorded from the Source (red) and from Target (blue) differ, depending on where the stimulus is delivered. Putative axonal, synaptic, and integration delays become apparent in **(A)** but not in **(B)**, suggesting a preferred synaptic connectivity (i.e., from Source to Target) exist. **(C-D)** Under control conditions (i.e., with no PDMS device), evoked responses detected at two distinct sets of MEA microelectrodes do not depend on the stimulus delivery location. The pale-hued shading, enveloping the lines in the plots, denotes the instantaneous standard error of the mean (N stimuli = 150).

Please click here to view a larger version of this figure.

Solution Name	Composition
polyethyleneimine (PEI) 0.1%	1 mL of PEI stock solution, 9 mL of sterile deionized (DI) water.
Culture medium (50 mL)	Minimum Essential Medium (MEM), supplemented by 20 µM Glucose, 50 µg/mL Gentamicin, 50 µM L-glutamine, and, 10% Heat-Inactivated Horse Serum.
Dissection medium (1000 mL)	Hanks′ Balanced Salts 9.52 g, Sodium bicarbonate 350 mg, HEPES 2.83 g, D-(+)-Glucose 6 g, Kynurenic acid (final concentration 200 µM), D-AP5 (final concentration 25 µM), Gentamicin 250 µl, Bovine Serum Albumin 300 mg, Magnesium sulfate 1.44 g. Adjust the pH to 7.3, protect from light and store at 4°C.
Digestion medium (100 mL)	Sodium chloride 800 mg, Potassium chloride 37 mg, di-Sodium hydrogen phosphate 99 mg, HEPES 600 mg, Sodium bicarbonate 35 mg, Kynurenic acid, 200 µL (from 100 mM stock), D-AP5 100 µL (from stock 25 mM). Adjust the pH to 7.4, protect from light and store at 4 °C.
Solution 1	Trypsin 5 mg, Deoxyribonuclease I 1.5 mg, in 2 mL of Digestion medium.
Solution 2	Trypsin inhibitor 5 mg, in 5 mL of Dissection medium.
Solution 3	Deoxyribonuclease I 1.5 g, in 2.5 mL of Dissection medium.

Table 1: Table of solutions. Refer to the table of materials for product descriptions.

Supplementary Coding File 1: The STL design file corresponds to the structure depicted in **Figure 2A**. Please click here to download this File.

Discussion

Despite being decades-old, the application of 2PP technology in micrometer-scale PDMS-based replica molding is a recent development[43,44]. In this context, a series of points are discussed below to assist users in effectively reproducing this work.

For 3D model design, ensure that the model does not have holes or self-intersections. Privilege the binary file format when saving as STL, for its smaller file size footprint than ASCII-encoded. This is especially beneficial for designs with intricate geometries and for milliliter-wide objects. Using binary STL files also implies low CPU load, later in the process preparing the mechanical part to be 3d-printed**.** The features' physical dimensions within the STL file are represented in dimensionless units. During postprocessing the STL file, units are interpreted as micrometers. Therefore, it is recommended to adopt upfront the unit of interest, i.e., micrometer, when preparing the file. The accuracy of the printed model is determined by the number of surfaces approximating tessellated triangles. For an insufficient number of surfaces, undesired surface roughness will emerge. Nonetheless, aiming for excessively high accuracy by a very large number of surfaces comes at the price of a high computational load, causing the file processing to be slow.

For 3D printing, during printing, the 3D physical object is formed using fast galvo scanning in the x-y plane and piezo

motion in the z-direction. This focuses the femtosecond laser beam within any given 3D voxel. However, when printing structures are larger than the galvo's and piezo's spatial coverage ranges, the object must be programmatically split into blocks. While this a requirement for millimeter-sized printed parts, junctions among blocks are associated to (imperfect) stitching lines. Careful optimization of blocks count and placement of stitching lines in x, y, and z directions are crucial to avoid disrupting critical geometrical features of the final object with stitching lines. Bubbles may form at the printing interface for various reasons (e.g., substrates photoresist's impurities and inhomogeneities), and negatively impact the quality and integrity of the printed structure. Moreover, higher laser power can lead to an increase in their occurrence. Reducing the laser power, at the lowest layer of the printed part, will minimize the chances of bubble formation. As an alternative to printing the entire part as a solid structure, shell- and-scaffold method can be considered. It involves printing only the outer surface of the part (shell) as well as triangular prism elements within it. These elements are separated by horizontal layers (scaffold), holding the unpolymerized resin in small pockets. This method significantly shortens the printing time, relevant particularly for millimeter-sized structures. However, as non-polymerized resin remains, post-printing UV exposure is imperative to ensure full mechanical stability, although this step must be performed gently to avoid any deformation of the printed part. Post-curing time depends on the resin of choice, part's thickness, and UV power[40]. For optimal results, it is recommended to conduct an initial trial to estimate the time needed for full-depth curing, using a drop of photoresist and evaluating its section-cut, following UV exposure. The usual curing period ranges between 5 to 20 min.

For PDMS replica molding, clean fabrication of a PDMS device with micrometer-scale features, with no clean-room facilities, can be challenging: air-borne micro-particles can reside on the highly adhesive surface of the PDMS and hinder the seal between the device and substrate, or block the section of individual microchannels. Performing the protocol steps under a laminar flow hood and consistently shielding the PDMS surface with isopropanol substantially minimizes the contamination risks. The curing temperature and its duration directly affect PDMS cross linking and the resulting physical properties. In particular, the adhesiveness of cured PDMS is a critical factor. On the one hand, a tight seal is required between the PDMS device, and the surface used for neuronal cell culturing (e.g., a glass coverslip or a MEA), to effectively restrict the passage of the neurites. On the other hand, the PDMS device should attach to the surface reversibly, so that the delicate insulating layer MEAs is not damaged after removing the device. While PDMS shrinkage during curing occurs and might be corrected by upfront rescaling the mold, for temperatures and curing intervals indicated here shrinkage will be less than 2%[42] and will not affect significantly, single-layered PDMS devices. Overall, precisely follow the recommended curing temperature and duration values, for the best results.

Overview of advantages and limitations of the method

A technique based on 2-photon direct laser writing is proposed for the rapid fabrication of micro-scale polymeric devices for the experimental study of modular neural networks. As opposed to soft photolithography, the proposed approach does not require a high level of technical expertise, provided a functional 2PP 3D printing setup is accessible and operational. Remarkably, the method enables going from a CAD-designed 3D model to a functional PDMS device within a single day, thus providing a direct and

efficient path from concept to tangible realization. Specifically, opting for the shell-and-scaffold printing mode significantly reduces the time needed to create the mold, as only a fraction of its volume is printed. Subsequent UV-curing of the printed component guarantees its mechanical stability and robustness, as verified here over 50 casting cycles with PDMS.

Compared to traditional methods, 2PP 3D printing boasts a clear advantage, which is most pronounced when it comes to the fabrication of molds with a significant aspect ratio, demanding resolution requirements, and complex three-dimensional geometries. The production of master molds using standard UV lithography is constrained by a resist thickness of approximately 200 µm. Intricate sequences of spin-coating and exposure cycles[35], costly LIGA (Lithography, Electroplating, and Molding), or deep reactive ion etching (DRIE) processes[36] are required to achieve greater height and aspect ratios. In sharp contrast, as demonstrated in the pioneering work of Kumi et al. in 2010[37], the 2PP technique offers an essentially limitless scope for the aspect ratio of the printed parts, spanning from sub-micrometer to millimeters. Here, the micromanufacturing process of a mold with significant difference in height of its portions has been exemplified, featuring over a 100-fold distinction between the microchannels' height (5 µm and the maximum mold's height (545 µm; see **Figure 2**).

Also, sub-micrometer resolution could be readily achieved by following the protocol specifications outlined. In comparison, achieving enhanced mold resolutions through UV photolithography demands capital investment. The masks with the finest resolution, utilizing chromium deposition on quartz at a nominal resolution of 600 nm, are priced several orders of magnitude higher than the laser-printed overhead transparency masks, which possess a resolution of 250 µm[35], however see the work of Pirlo et al.[41]. To be viable for in-house use, a chosen method must be cost-effective. For many biological laboratories, the overall expense associated with conventional soft photolithography or direct laser writing presents a barrier. While it is feasible to make both technologies more accessible by purchasing and assembling the essential components, this approach demands additional expertise and still requires a notable investment. In this context, an essential point to consider is the broader spectrum of applications achievable through direct laser writing. Unlike conventional soft photolithography, primarily limited to mold micromanufacturing, 2PP 3D printing exhibits remarkable versatility. Its potential applications span from microfluidics and micro-optics to integrated photonics and micromechanics. This makes investing in this technology appealing as a shared facility for multiple and diverse scientific fields. For instance, the 2PP based methodology devised in this protocol is the result of an interdisciplinary collaboration between neuroscience and mathematics departments within our institution. Additionally, the photoresist development is an active field of research, and can potentially expand the range of applications of 2PP 3D printing. A case in point is the recent introduction of IP-PDMS resin. By polymerizing into structures with properties like PDMS[38], this resin unlocks the potential for direct microfabrication of biocompatible components that have convoluted surface or contains hollow spaces. These intricacies stand as barriers to achieving similar outcomes through conventional replica molding procedures.

As a demonstration of this method, evidence was provided suggesting the development of unidirectional connectivity between two modules in a modular neuronal network. The micro-scale mold, manufactured by 2PP technique, had

enough endurance to undergo multiple PDMS casting, and has the required micro-scale precision. In conclusion, the scope of application of the protocol described in this work extends beyond the case illustrated. As access to the 2PP printing technology becomes increasingly widespread, the initial investment required for its implementation will decrease while its range of potential applications will expand.

Disclosures

The authors have nothing to disclose.

Acknowledgments

M.G. acknowledges financial support from the European Union's H2020 Framework Programme through the European Innovation Council (IN-FET project, GA n. 862882, Arbor-IO project, FLAG-ERA and the Human Brain Project, ID 650003) and from SISSA (Neuroscience Area). G.N. acknowledges financial support from the Italian Ministry of University and Research (MUR) through the grant Dipartimenti di Eccellenza 2018-2022 (Mathematics Area). We thank M. Gigante, B. Pastore, and M. Grandolfo for their assistance with 3D printing, cell culturing, and live-imaging, as well as Drs. P. Massobrio, P. Heppenstall, L. Ballerini, Di Clemente, and H.C. Schultheiss for discussions. The funders had no role in study design, data collection and analysis, decision to publish, or preparation of the manuscript.

References

1. Kanagasabapathi, T. T. et al. Dual-compartment neurofluidic system for electrophysiological measurements in physically segregated and functionally connected neuronal cell culture. *Front Neuroeng.* **4**, 13 (2011).
2. Maeda, E., Robinson, H. P. C., Kawana, A. The mechanisms of generation and propagation of synchronized bursting in developing networks of cortical neurons. *J Neurosci.* **15** (10), 6834-6845 (1995).
3. Wheeler, B. C., Brewer, G. J. Designing neural networks in culture. *Proc IEEE Inst Electr Electron Eng.* **98** (3), 398-406 (2010).
4. DeMarse, T. B., Pan, L., Alagapan, S., Brewer, G. J., Wheeler, B. C. Feed-forward propagation of temporal and rate information between cortical populations during coherent activation in engineered in vitro networks. *Front Neural Circuits.* **10**, 32 (2016).
5. Kanagasabapathi, T. T. et al. Functional connectivity and dynamics of cortical-thalamic networks co-cultured in a dual compartment device. *J Neural Eng.* **9** (3), 036010 (2012).
6. Brofiga, M., Pisano, M., Tedesco, M., Raiteri, R., Massobrio, P. Three-dimensionality shapes the dynamics of cortical interconnected to hippocampal networks. *J Neural Eng.* **15** (5), 056044 (2020).
7. Bisio, M., Bosca, A., Pasquale, V., Berdondini, L., Chiappalone, M. Emergence of bursting activity in connected neuronal sub-populations. *PLoS One.* **9** (9), e107400 (2014).
8. Hasan, M. F., Berdichevsky, Y. Neural circuits on a chip. *Micromachines.* **7** (9), 157 (2016).
9. Aebersold, M. J. et al. "Brains on a chip": Towards engineered neural networks. *TrAC Tren Anal Chem.* **78**, 60-69 (2016).
10. Zamora-López, G., Chen, Y., Deco, G., Kringelbach, M. L., Zhou, C. Functional complexity emerging from anatomical constraints in the brain: The significance of

network modularity and rich-clubs. *Sci Rep.* **6**, 38424 (2016).

11. Eytan, D., Marom, S. Dynamics and effective topology underlying synchronization in networks of cortical neurons. *J Neurosci.* 26 (33), 8465-8476 (2006).
12. Pan, L., Alagapan, S., Franca, E., Brewer, G.J., Wheeler, B. C. Propagation of action potential activity in a predefined microtunnel neural network. *J Neural Eng.* **8** (4), 046031 (2011).
13. Virlogeux, A. et al. Reconstituting corticostriatal network on-a-chip reveals the contribution of the presynaptic compartment to Huntington's disease. *Cell Rep.* **22** (1), 110-122 (2018).
14. Kleinfeld, D., Kahler, K., Hockberger, P. E. Controlled outgrowth of dissociated neurons on patterned substrates. *J Neurosci.* **8** (11), 4098-4120 (1988).
15. Vogt, A. K., Wrobel, G., Meyer, W., Knoll, W., Offenhäusser, A. Synaptic plasticity in micropatterned neuronal networks. *Biomaterials.* **26** (15), 2549-2557 (2005).
16. Staii, C. et al. Positioning and guidance of neurons on gold surfaces by directed assembly of proteins using atomic force microscopy. *Biomaterials.* **30** (20), 3397-3404 (2009).
17. Fricke, R. et al. Axon guidance of rat cortical neurons by microcontact printed gradients. *Biomaterials.* **32** (8), 2070-2076 (2011).
18. Gladkov, A. et al. Design of cultured neuron networks in vitro with predefined connectivity using asymmetric microfluidic channels. *Sci Rep.* **7** (1), 15625 (2017).
19. le Feber, J., Postma, W., de Weerd, E., Weusthof, M., Rutten, W. L. Barbed channels enhance unidirectional connectivity between neuronal networks cultured on multi electrode arrays. *Front Neurosci.* **9**, 412 (2015).
20. Peyrin, J. M. et al. Axon diodes for the reconstruction of oriented neuronal networks in microfluidic chambers. *Lab Chip.* **11** (21), 3663-3673 (2011).
21. Xia, Y., Whitesides, G. M. Soft lithography. *Angewandte Chemie - International Edition.* **37** (5), 550-575 (1998).
22. Qi, D., Hoelzle, D. J., Rowat, A. C. Probing single cells using flow in microfluidic devices. *Eur Phys J Spec Top.* **204**, 85-101 (2012).
23. Brower, K., White, A. K., Fordyce, P. M. Multi-step variable height photolithography for valved multilayer microfluidic devices. *J Vis Exp.* (119), 55276 (2017).
24. Levis, M., Ontiveros, F., Juan, J., Kavanagh, A., Zartman, J. J. Rapid fabrication of custom microfluidic devices for research and educational applications. *J Vis Exp.* (153), 60307 (2019).
25. Maruo, S., Nakamura, O., Kawata, S. Three-dimensional microfabrication with two-photon-absorbed photopolymerization. *Opt Lett.* **22** (2), 132-134 (1997).
26. Baldacchini, T. *Three-dimensional microfabrication using two-photon polymerization: Fundamentals, technology, and applications.* Elsevier (2015).
27. Madou, M. J. *Fundamentals of Microfabrication.* CRC Press (2018).
28. Sun, H. B., Kawata, S. Two-photon photopolymerization and 3D lithographic microfabrication. *NMR, 3D Anal, Photopolymeriz. Adv Poly Sci.* **170**, 169-273 (2004).
29. Marom, S., Shahaf, G. Development, learning and memory in large random networks of cortical neurons: Lessons beyond anatomy. *Q Rev Biophys.* **35** (1), 63-87 (2002).

30. Kamioka, H., Maeda, E., Jimbo, Y., Robinson, H. P. C., Kawana, A. Spontaneous periodic synchronized bursting during formation of mature patterns of connections in cortical cultures. *Neurosci Lett.* **206** (2-3), 109-112 (1996).

31. Hales, C. M., Rolston, J. D., Potter, S. M. How to culture, record and stimulate neuronal networks on micro-electrode arrays (MEAs). *J Vis Exp.* (39), 2056 (2010).

32. Mahmud, M., Pulizzi, R., Vasilaki, E., Giugliano, M. QSPIKE tools: A generic framework for parallel batch preprocessing of extracellular neuronal signals recorded by substrate microelectrode arrays. *Front Neuroinform.* **8**, 26 (2014).

33. Pulizzi, R. et al. Brief wide-field photostimuli evoke and modulate oscillatory reverberating activity in cortical networks. *Sci Rep.* **6** (1), 24701 (2016).

34. Scarsi, F., Tessadori, J., Chiappalone, M., Pasquale, V. Investigating the impact of electrical stimulation temporal distribution on cortical network responses. *BMC Neurosci.* **18** (1), 49 (2017).

35. Friend, J., Yeo, L. Fabrication of microfluidic devices using polydimethylsiloxane. *Biomicrofluidics.* **4** (2), 026502 (2010).

36. Kim, K. et al. Rapid replication of polymeric and metallic high aspect ratio microstructures using PDMS and liga technology. *Microsystem Technologies.* **9** (1-2), 5-10 (2002).

37. Kumi, G., Yanez, C. O., Belfield, K. D., Fourkas, J. T. High-speed multiphoton absorption polymerization: Fabrication of microfluidic channels with arbitrary cross-sections and high aspect ratios. *Lab Chip.* **10** (8), 1057-1060 (2010).

38. Bunea, A. I. et al.Micro 3D printing by two-photon polymerization: Configurations and parameters for the nanoscribe system. *Micro.* **1** (2), 164-180 (2021).

39. Taylor, A. et al. A microfluidic culture platform for CNS axonal injury, regeneration and transport. *Nat Methods.* **2** (8), 599-605 (2005).

40. Oakdale, J. S, Ye, J., Smith, W. L., Biener, J. Post-print UV curing method for improving the mechanical properties of prototypes derived from two-photon lithography. *Opt. Express.* **24** (24), 27077-27086 (2016).

41. Pirlo, R. K., Sweeney, A. J., Ringeisen, B. R., Kindy, M., Gao, B. Z. Biochip/laser cell deposition system to assess polarized axonal growth from single neurons and neuron/glia pairs in microchannels with novel asymmetrical geometries. *Biomicrofluidics.* **5** (1), 13408 (2011).

42. Madsen, M. H., Feidenhans'l, N. A., Hansen, P. E. Garnæs, J., Dirscherl, K. Accounting for PDMS shrinkage when replicating structures. *J Micromech Microeng.* **24** (12), 127002 (2014).

43. Comina, G., Suskaa, A., Filippini, D. PDMS lab-on-a-chip fabrication using 3D printed templates. *Lab Chip.* **14** (2), 424-430 (2013).

44. Chan, H. N. et al. Direct, one-step molding of 3D-printed structures for convenient fabrication of truly 3D PDMS microfluidic chips. *Microfluid Nanofluid.* **19**, 9-18 (2015).